

Dynamics and chaotic properties of the fully disordered Kuramoto model

Iván León¹ and Diego Pazó²¹*Departamento de Matemática Aplicada y Ciencias de la Computación, Universidad de Cantabria, Santander, Spain,*²*Instituto de Física de Cantabria (IFCA), Universidad de Cantabria–CSIC, 39005 Santander, Spain*

(Dated: 8 July 2025)

Frustrated random interactions are a key ingredient of spin glasses. From this perspective, we study the dynamics of the Kuramoto model with quenched random couplings: the simplest oscillator ensemble with fully disordered interactions. We answer some open questions by means of extensive numerical simulations and a perturbative calculation (the cavity method). We show frequency entrainment is not realized in the thermodynamic limit and that chaotic dynamics are pervasive in parameter space. In the weak coupling regime, we find closed formulas for the frequency shift and the dissipativeness of the model. Interestingly, the largest Lyapunov exponent is found to exhibit the same asymptotic dependence on the coupling constant irrespective of the coupling asymmetry, within the numerical accuracy.

A wide variety of natural and artificial systems are modeled as populations of interacting limit-cycle oscillators¹. Studying the emergent phenomena in these systems is a well-established research field. For simplicity, it is usual to consider one-dimensional (phase) oscillators since they capture the dynamics of limit-cycle attractors, provided the interactions are sufficiently weak². In this context, a prominent system is the Kuramoto model³, describing the transition to collective synchronization of heterogeneous phase oscillators under all-to-all attractive interactions. However, this is only the tip of the iceberg, as many other phenomena arise for other interaction schemes.

A particularly interesting situation arises when attractive and repulsive interactions are randomly spread in the population. In such a situation a complex behavior can be foreseen due to the so-called frustration, as occurs in spin-glass models⁴. Indeed, with the purpose of observing an ‘oscillator glass’ in 1992 Daido⁵ modified the Kuramoto model introducing random frustrated interactions. Arguably, his numerical simulations displayed a quasi-glassy phase. A few years later, Stiller and Radons⁶ generalized the model allowing the interactions to be nonsymmetric. Chaotic dynamics was shown to be preponderant in that case. Analytical descriptions, borrowing techniques from spin glass theory^{7–10}, and numerical studies^{11,12} have appeared in recent years. In spite of these advances, our understanding of the model remains quite limited.

In this paper we revisit the problem answering open questions and improving previous results. We resort to extensive numerical simulations, and the perturbative cavity method recently developed for this system^{9,10}. Our numerical simulations indicate that in the thermodynamic limit ($N \rightarrow \infty$), oscillators do not get entrained for any finite value of the parameters. Furthermore, we show the pervasiveness of chaotic dynamics in the thermodynamic limit. Specifically, for small coupling, the value of the largest Lyapunov exponent appears to be insensitive to the asymmetry of the coupling.

I. INTRODUCTION

Synchronization and other emergent phenomena in populations of oscillators have been profusely studied due to their relevance in many fields, from biology to engineering¹. The Kuramoto model^{2,3} stood out as a simple system capable of describing the transition to collective synchrony with minimal ingredients. In particular, the interactions between the (phase) oscillators were chosen global, uniform, and pairwise, and the only source of disorder is provided by the heterogeneous natural frequencies. Along the years, these simplifying assumptions have been relaxed in different ways: including more sophisticated forms of disorder^{13–18} or setting complex coupling topologies, like random networks^{19,20} or the actual human-brain connectome network²¹.

Decades ago, motivated by the complex behavior of spin glasses, a modified Kuramoto model with fully disordered interactions (of Sherrington-Kirkpatrick type⁴) was put forward by Daido⁵. He reported the existence of an ‘oscillator glass’, a state displaying “quasientrainment”⁵, as well as slow (algebraic) relaxation to the asymptotic state^{5,22,23}. In Ref. 5, it was argued that such quasi-glassy state was concomitant with a concave up density of local fields at zero; a “volcano state” in the recent jargon²⁴. In recent works the volcano transition was studied adopting a low-rank coupling matrix^{11,24}. Borrowing techniques from spin-glass theory, the genuine full-rank coupling matrix was studied^{7,8} and led to a rigorous analysis of the volcano transition by means of a perturbative approach^{9,10}.

The model proposed by Daido assumed symmetric (i.e. reciprocal) interactions. This restriction, grounded in physical laws for magnetic interactions, is unrealistic in many other domains. Indeed, the effect of nonreciprocity has been investigated in several disordered systems. While some systems^{25,26} show robust spin-glass features, in other systems the spin-glass phase is fragile²⁷. Stiller and Radons analyzed the Daido model with asymmetric interactions⁶, concluding that chaos was generic in the model. (Incidentally, chaos is also observed in similar models of coupled oscillators with phase-lag disorder¹⁷.) However, Stiller and Radons also reported that a region with non-chaotic behavior, denoted

as “freezing”, survived for weak nonreciprocity and large enough coupling.

In this paper, we revisit the Daido-Stiller-Radons (DSR) model, in an attempt to clarify certain questions: Is quasi-entrainment (frequency entrainment without phase locking) real? Which is the exact domain of chaos? Is non-chaotic behavior robust against weak non-reciprocities and heterogeneity? Our work provides answers to these questions, and at the same time, it points to an apparent universal scaling of chaos in the weak coupling regime. Moreover, we obtain an asymptotic law for the dissipativeness of the model in the weak coupling regime.

This paper is organized as follows. In section II we introduce the studied model. We provide a brief survey of the observed phenomenology and customary methodologies in Sec. III. Sections IV and V are devoted to the study of the dynamics and Lyapunov exponents on two special limits of the model, weak and infinitely strong coupling. Then we complete the picture in Sec. VI by analyzing the moderate and strong coupling regimes. Finally, we present the conclusions in Sec. VII.

II. MODEL

In this paper we consider the Kuramoto model with quenched random interactions or Daido-Stiller-Radons (DSR) model, for short. It consists of N oscillators, with their phases $\{\theta_j\}_{j=1,\dots,N}$ governed by the differential equations:

$$\frac{d\theta_j}{dt} \equiv \dot{\theta}_j = \omega_j + \frac{J}{\sqrt{N}} \sum_{k=1}^N K_{jk} \sin(\theta_k - \theta_j). \quad (1)$$

The intrinsic frequencies $\{\omega_j\}$ are independently drawn from a normal distribution $g(\omega)$ with variance σ^2 and zero mean (by going to a rotating frame, if necessary). The heterogeneous couplings are encoded in the matrix elements K_{jk} , drawn from a zero-mean unit-variance normal distribution (diagonal elements vanish: $K_{jj} = 0$). The correlation between diagonally opposed matrix elements is:

$$\langle K_{jk} K_{kj} \rangle = \eta \quad (j \neq k). \quad (2)$$

The parameter $\eta \in [-1, 1]$ controls the reciprocity of the coupling. The specific values $\eta = 1, 0$ and -1 correspond to reciprocal, fully asymmetric, and anti-reciprocal coupling, respectively. The dynamics of the model (1) also depends on the coupling constant J . We have, in sum, a set of ODEs with $N(N-1)$ quenched random coefficients K_{jk} and N random natural frequencies ω_j . For large enough N we can focus on “typical” behaviors controlled by three continuous parameters: σ , J and η .

For future discussion, we cast system (1) with each oscillator driven by its own local field:

$$\dot{\theta}_j = \omega_j + J r_j \sin(\psi_j - \theta_j), \quad (3a)$$

$$r_j e^{i\psi_j} = \frac{1}{\sqrt{N}} \sum_{k=1}^N K_{jk} e^{i\theta_k} \quad (3b)$$

It is important to notice that only the ratio between σ and J matters. Introducing a rescaled time $\tau = Jt$, and expressing the natural frequencies as $\omega = \sigma\tilde{\omega}$, with $\tilde{\omega}_j \sim \mathcal{N}(0, 1)$, the model becomes:

$$\frac{d\theta_j}{d\tau} = \frac{\sigma}{J} \tilde{\omega}_j + \frac{1}{\sqrt{N}} \sum_{k=1}^N K_{jk} \sin(\theta_k - \theta_j). \quad (4)$$

Written in this form it is clear that there are only two relevant continuous parameters in the model: the rescaled frequency dispersion σ/J , and the asymmetry of the coupling η . Nevertheless, it is important to keep in mind the other ingredients: the population size N , the particular realization of the disorder, and the initial condition for the phases.

It will be also convenient to refer to an alternative representation of the model:

$$\frac{d\theta_j}{dT} = \tilde{\omega}_j + \frac{J/\sigma}{\sqrt{N}} \sum_{k=1}^N K_{jk} \sin(\theta_k - \theta_j). \quad (5)$$

Now the rescaled time is $T = \sigma t$.

III. BACKGROUND

Once the DSR model has been properly introduced, it is convenient to review its main properties. We will first focus on its phenomenology. The specific methodologies to tackle the model are afterwards introduced.

A. Phenomenology

In the original works by Daido⁵ and Stiller and Radons⁶ certain novel phenomena arising in Eq. (1) were described. In what follows we briefly comment on these phenomena and the current understanding of them.

1. Glassy phase at zero temperature

To contextualize the phenomenology of the DSR model, we first revisit the limiting case of identical oscillators ($\sigma = 0$) and reciprocal interactions ($\eta = 1, J \neq 0$). In this particular case the phases obey gradient dynamics:

$$\dot{\theta}_j = -\frac{\partial V}{\partial \theta_j}, \quad (6)$$

with potential

$$V(\theta) = -\frac{J}{\sqrt{N}} \sum_{j=1}^{N-1} \sum_{k=j+1}^N K_{jk} \cos(\theta_k - \theta_j). \quad (7)$$

In turn, the system eventually settles into a resting state, i.e. a stable fixed point, among an exponential number (with

N) of them due to the frustrated interactions²⁸. The relaxation process of the global order parameter

$$|Z| = \frac{1}{N} \left| \sum_k^N e^{i\theta_k} \right| \quad (8)$$

turns out to be “superslow” ($\sim 1/\ln t$), according to the numerical results in Ref. 29.

2. Volcano transition

The question whether the just described glassy phase is robust for nonzero σ (in analogy to the persistence of magnetic spin-glasses at finite temperature) motivated Daido⁵ to introduce and study the DSR model (with $\eta = 1$). It is important to notice that for nonzero σ the DSR model loses its gradient character. Daido found that, above a critical coupling J_v , the density $\rho(r)$ of the local-field amplitudes, see Eq. (3b), becomes concave up at zero. (Recent numerical estimations of the critical coupling are $J_v \approx 1.3\sigma^{9,11}$.) Hence the local fields organize like a volcano in the complex plane. Daido argued the volcano phase was concomitant with the quasientrainment between the oscillators, and the algebraic relaxation of $|Z|$ (see below).

3. Slow relaxation

The algebraic decay to 0 of the global order parameter (8) was presented in Ref. 5 as a signature of a “quasi-glassy” state in the volcano phase. This fact drew some controversy^{6,22,23}, in part because the average over coupling matrices can be inside or outside the absolute value. Prüser et al.⁹ recently argued that the volcano transition cannot be linked to the glassy transition. However, recent numerical simulations with $N = 10^4$ oscillators¹² support the algebraic decay of $|Z|$ in the volcano phase. If the onset of this algebraic decay coincides with $J = J_v$ deserves further scrutiny since, according to Ref. 12, it shows up only if the coupling is progressively increased with N as $J \sim \sqrt{N}$.

4. Quasientrainment

Another phenomenon observed in the volcano phase was the quasientrainment of oscillators⁵. It consisted in an apparent frequency locking of some oscillators, but with their phases diffusing (i.e., no phase-locking). Despite the puzzling character of this behavior in a deterministic system, it remains insufficiently explored in our opinion.

5. Freezing

Stiller and Radons observed a quasi-glassy state in the form of a frozen state for strong couplings, $J > J_f \approx 24$

(far beyond the volcano transition). Actually, the value of σ was not specified in Ref. 6, but we can presume $\sigma = 1$. Freezing was described as a state in which all oscillators became entrained to the central frequency. However, only small population sizes ($N = 100 - 400$) were studied, so this result might not hold in the thermodynamic limit.

6. The effect of nonreciprocity

The robustness of the previous phenomena against coupling asymmetry ($\eta < 1$) is an interesting question. Stiller and Radons⁶ concluded that a quasi-glassy (freezing) phase indeed persisted for $\eta_c(J) < \eta < 1$, with $\lim_{J \rightarrow \infty} \eta_c(J) \approx 0.8$. Again, this conclusion is supported by simulations with a small number of oscillators ($N = 100$), see Fig. 8 in Ref. 6.

Concerning the volcano phase, it was recently shown that it persists for non-reciprocal coupling¹¹. Specifically, the volcano exists in the range $\eta > \eta_v \approx 0.2$. This result is consistent with a recent perturbative calculation, valid for small J ¹⁰.

7. Chaos

Stiller and Radons also noticed that the model is chaotic outside the domain of freezing, i.e. in most of the (η, J) phase plane, see Fig. 8 in Ref. 6. Nevertheless a detailed analysis of the scaling of chaos was not pursued. In the standard Kuramoto model the Lyapunov exponent is known to scale quadratically with the coupling constant³⁰, but, to our knowledge, this remains unknown for the DSR model. We end noting that the volcano phase may perfectly coexist with chaos, while freezing and chaotic dynamics are mutually exclusive.

B. Methodologies

The DSR can be analyzed following two main complementary strategies: direct numerical simulations and self-consistent methods. The advantages of each approach depends on the features under study.

The direct numerical integration of the model, Eq. (1), for fixed parameters and number of oscillators is the more straightforward approach. It was exclusively used in Refs. 5, 11, 22, and 23, and partly used in Refs. 6 and 12. Any dynamical quantity can be computed numerically, though finite-size effects are unavoidable. Keeping these effects sufficiently small entails a severe computational cost. All the numerical simulations in this paper use this straightforward method. The reference value $\sigma = 1$ is adopted, unless otherwise stated. The numerical integration was performed with a fourth-order Runge-Kutta algorithm of time step:

$$\Delta t = \min(0.1, 0.5/J)$$

(or smaller in certain cases). The frequencies could be drawn at random or deterministically sampled from $g(\omega)$ with no effect in any of the results of this paper.

A second approach is to consider self-consistent dynamic mean-field and cavity methods as in Refs. 6, 9, 10, and 31. They adopt the thermodynamic limit from the outset, reducing the infinite set of ODEs to a self-consistent single-site problem, i.e., a stochastic equation for one oscillator driven by self-consistent noises. This self-consistent problem can be analytically solved perturbatively for weak coupling^{9,10}. However, for general coupling, the numerical self-consistence of noise is achieved iteratively. To deal with the heterogeneity of frequencies, noise is obtained averaging over M different noisy oscillators of frequencies $\{\omega_i\}_{i=1,\dots,M}$, introducing in this way $O(1/\sqrt{M})$ finite-size effects³¹. Notice, nevertheless, that the scaling of the fluctuations is known in contraposition to the less controllable N -dependent fluctuations of direct numerical simulations.

The self-consistent method has shown its utility at computing the decay of the order parameter⁶, noise correlations³¹ and the weak coupling dynamics^{9,10}. However there is a caveat: Lyapunov exponents cannot be computed using this approach; the evolution of an infinitesimal perturbation cannot be computed self-consistently. This imply that to study the nature of chaos, our only viable alternative is direct numerical simulation.

We briefly comment on a third approach: the study of low-rank models. These are models of the form of Eq. (1) where the coupling matrix K is a random matrix with low rank^{24,32}, such that when the rank tends to infinity it converges to K as defined in Eq. (2)¹¹. If the rank is much smaller than the number of oscillators, those models can be solved through the Ott-Antonsen theory. Unfortunately, the conclusions derived from low-rank models do not generically apply to the full-rank model. The absence of algebraic relaxation²⁴ and the disparate values of critical asymmetry for the volcano transition¹¹ illustrate the limitations of low-rank models.

IV. WEAK COUPLING

We initially consider weak coupling. As a reference value, we recall that the volcano transition occurs at $J_v \approx 1.3\sigma$ for $\eta = 1$ (after proper rescaling of the recent numerical determination in Ref. 11, see also 9). Therefore it is reasonable to identify the parameter region $J/\sigma \leq 1$, as the weak coupling regime.

A. Long-term average frequencies

Repulsive and attractive interactions are equally present in the DSR model. It is therefore not obvious at first sight if the oscillators should exhibit a tendency to approach their actual frequencies or not. The average frequencies $\Omega_j = \langle \theta_j \rangle_t$ are the first subject of our work.

Numerical simulations of Eq. (1) were carried out with $N = 10^4$ oscillators, setting $\sigma = 1$, and choosing different

combinations of $J = \{0.1, 1\}$ and $\eta = \{-1, 0, 1\}$. Multiple realizations of the coupling matrix and initial conditions were also implemented but no quantitative difference was noticeable. The average frequencies Ω_j were computed over $t = 10^5$ time units. The results for the set of 6 combinations of parameters η and J are depicted in Fig. 1. We found convenient to represent the displacement of the frequency $\Omega_j - \omega_j$ against ω_j . As each panel has a different scale in the y -axis, we always include, as a reference, a dotted straight line corresponding to $\Omega_j = 0$ (the main frequency of entrainment, if it existed).

The upper panels of Fig. 1 correspond to a coupling constant $J = 0.1$, a rather small value. We see that, as J is increased from zero, the average frequencies move from ω_j towards 0, save in the anti-reciprocal case ($\eta = -1$). In the latter case the average frequencies remain mostly unperturbed by the coupling $\Omega_j \approx \omega_j$.

The bottom panels of Fig. 1 show the results for a larger coupling, $J = 1$. The Ω_j become even closer to 0, specially those with small $|\omega_j|$. Again this frequency displacement heavily depends on η . No trace of a frequency plateau is apparent, so oscillators are not entrained to any frequency.

By using the cavity method^{9,10} we can obtain Ω_j as a perturbative expansion in the small parameter J , see Appendix A. At the first non-trivial order in J we obtain:

$$\Omega_j = \omega_j - J^2 \frac{1+\eta}{\sqrt{2}} D_w(\omega_j/\sqrt{2}) + O(J^4), \quad (9)$$

where $D_w(x) = \exp(-x^2) \int_0^x \exp(y^2) dy$ is the so-called Dawson function. We see that the leading correction to ω_j is of order J^2 . (The next order is $O(J^4)$ since odd powers of J are absent due to the symmetry of the model under $J \rightarrow -J$.) Moreover, the prefactor $(1+\eta)$ implies maximal (null) frequency drift for $\eta = 1$ (-1). The function in Eq. (9) is represented by a dashed line in all panels of Fig. 1. The agreement between Eq. (9) and the numerical results in Fig. 1 for $J = 0.1$ is good. For $J = 1$ the numerical results exhibit a clear deviation from the asymptotic formula (9) (save for $\eta = -1$), although they are qualitatively similar. The discrepancies at $J = 1$ are not surprising, since Eq. (9) is a perturbative result, which already yields an unphysical non-monotonic dependence of Ω on ω for $J > \sqrt{2}$ ($\eta = 1$).

We close this section noting that the numerical data do not fall on a line, but form a ‘‘cloud’’ due to the finiteness of the population. The width of this cloud decreases with the number of oscillators as $1/\sqrt{N}$ (not shown), converging to a line in the thermodynamic limit.

B. Scaling of the dissipation

A theoretical analysis of the Lyapunov spectrum³³ of the DSR model is challenging. Infinitesimal perturbations obey the following linear equations:

$$\delta\dot{\theta}_j = \frac{J}{\sqrt{N}} \sum_{k=1}^N K_{jk} \cos(\theta_k - \theta_j) (\delta\theta_k - \delta\theta_j). \quad (10)$$

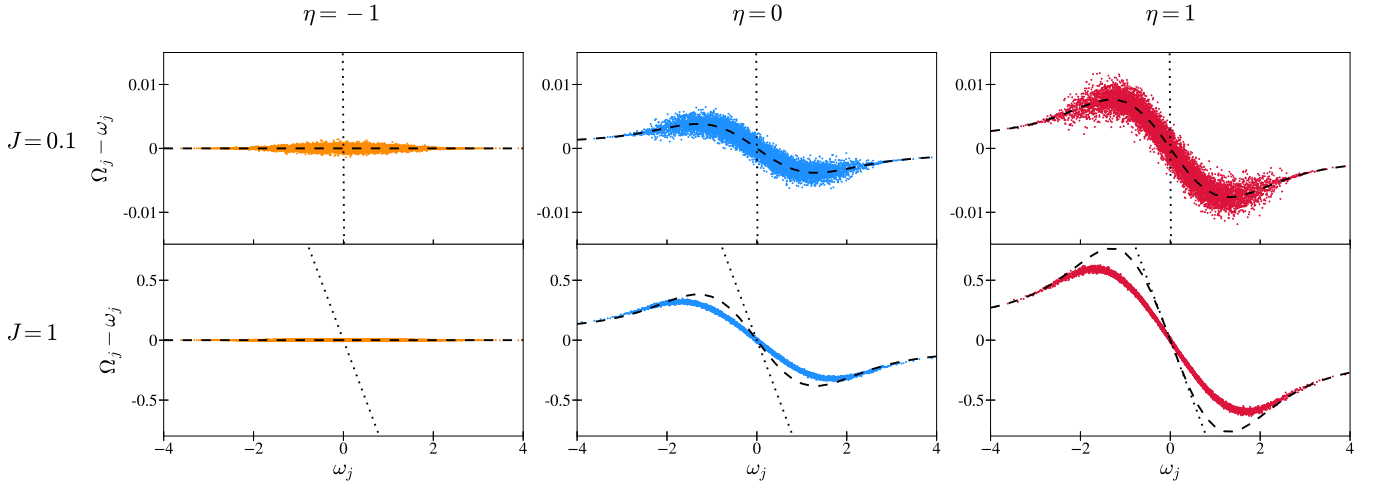


FIG. 1. Difference between average and natural frequencies versus the natural frequency, for $N = 10^4$ oscillators. In the upper (lower) row the coupling strength is fixed to $J = 0.1$ ($J = 1$). From left to right, the three columns correspond to $\eta = -1, 0$ and 1 , respectively. The dashed line indicates the perturbative theoretical result in Eq. (9). The straight dotted line indicates the vanishing long-term average frequency ($\Omega_j = 0$).

We can gauge the difficulties of achieving a theoretical result for the Lyapunov exponents, if we take into account that the problem still remains partly solved in the standard Kuramoto model, see Refs. 30, 34, and 35.

Seeking a theoretical result, it is more productive to focus on the average phase-space volume contraction rate per degree of freedom \mathcal{S} . This quantity measures the dissipativeness of the model, and equals the time average of the trace of the Jacobian matrix, see (10), divided by N . Or, written in mathematical form:

$$\mathcal{S} = -\frac{J}{N^{3/2}} \left\langle \sum_{jk}^N K_{jk} \cos(\theta_k - \theta_j) \right\rangle_t. \quad (11)$$

It is well known that \mathcal{S} equals the sum of the Lyapunov exponents³³ divided by N . We note that the finiteness of \mathcal{S} is compatible with the presence of extensive chaos.

For an antisymmetric coupling matrix ($\eta = -1$) it is immediate from the form of (11) that $\mathcal{S} = 0$; i.e. the dynamics is conservative, as previously pointed out in Refs. 6 and 36. For general η we can compute \mathcal{S} perturbatively, by means of the cavity method:

$$\mathcal{S} = -(1 + \eta) \frac{\sqrt{\pi}}{4} J^2 + O(J^4) \quad (12)$$

see appendix A for details. A log-log plot of this parabolic function is shown in Fig. 2 (a) for three selected values of η . This figure also shows the results of direct numerical determination of \mathcal{S} , via Eq. (11) driven by Eq. (1), for $N = 5000$. The agreement between theory and simulation is remarkably good.

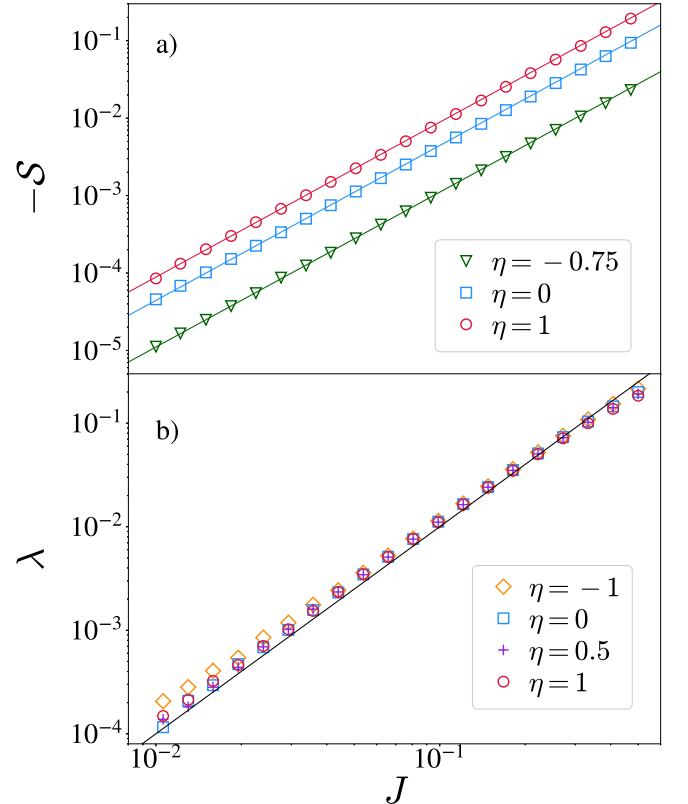


FIG. 2. (a) Log-log plot of the dissipation ($-\mathcal{S}$) versus J for different asymmetry parameters. The symbols correspond to numerical simulations with $N = 5000$ oscillators, and the solid lines are the theoretical result in Eq. (12). (b) Largest Lyapunov exponent versus J (in log-log scale) with $N = 2000$, for different asymmetry parameters. The black solid line is $\lambda = J^2$.

C. Scaling of the Lyapunov exponent

Here, we take a closer look at the dependence of the Lyapunov exponent on the coupling strength. In Fig. 2 (b), we depict the largest Lyapunov exponent λ versus J for $N = 2000$ oscillators and different values of η . The growth of the Lyapunov exponent is consistent with an asymptotic quadratic law:

$$\lambda(J \ll 1) \simeq cJ^2, \quad (13)$$

where “ \simeq ” denotes equality after neglecting marginal contributions in J , and c is a constant of order 1. Such a quadratic dependence on the coupling constant was already observed in the Kuramoto model³⁰, and other situations³⁷. A striking peculiarity of (13) is the apparent independence of the constant c on parameter η . The small deviations for small λ can be attributed to numerical accuracy. The insensitivity of λ to the value of η is particularly intriguing, since, as seen above, the average frequency and the dissipation do strongly depend on η .

The quadratic scaling of the Lyapunov exponent appears to be quite robust. We computed the Lyapunov exponent with a coupling matrix whose elements were drawn from a uniform distribution of unit variance. We obtained the quadratic scaling (13), with the same constant c (not shown), irrespective of the symmetry of the coupling matrix. These empirical observations suggest the quadratic scaling in Eq. (13) is the outcome of a general underlying mechanism at work in weakly coupled oscillators.

V. IDENTICAL FREQUENCIES (OR INFINITE COUPLING)

Now we focus on the limit opposite to the previous section. We set $\sigma = 0$, or equivalently $J \rightarrow \infty$, see Eqs. (4) and (5). This situation is already far from trivial.

Stiller and Radons concluded in Ref. 6 that the glassy state (freezing) persisted for $1 \geq \eta > \eta_c$, with $\eta_c(J \rightarrow \infty) \approx 0.8$. Our goal is inferring the behavior in the thermodynamic limit from the direct simulation of increasingly larger systems. To study the $J \rightarrow \infty$ limit it is convenient to set $\sigma = 0$, and a finite J value, e.g. $J = 1$. In Fig. 3 we represent the numerically determined Lyapunov exponent $\lambda_0(\eta)$. We averaged over independent realizations of the coupling matrix, and denote the ensemble mean by $[\lambda_0]$. Five different system sizes were considered. To make our results more reliable, $[\lambda_0]$ was computed both continuously increasing η (solid lines) and decreasing η (dashed lines), see Appendix B for details of the implementation. It is apparent that chaos persists for increasingly larger values of η as N grows. For $N = 3200$, the Lyapunov exponent (averaged over 10 independent realizations of the coupling matrix) approximately touches zero at $\eta_c \approx 0.9$, which is clearly above the estimation by Stiller and Radons. We conjecture that $\eta_c \rightarrow 1$ as $N \rightarrow \infty$, i.e. the glassy phase is fragile against weak nonreciprocity.

Let us end this section mentioning that, by trivial rescaling, a finite Lyapunov exponent λ_0 implies a linearly divergent

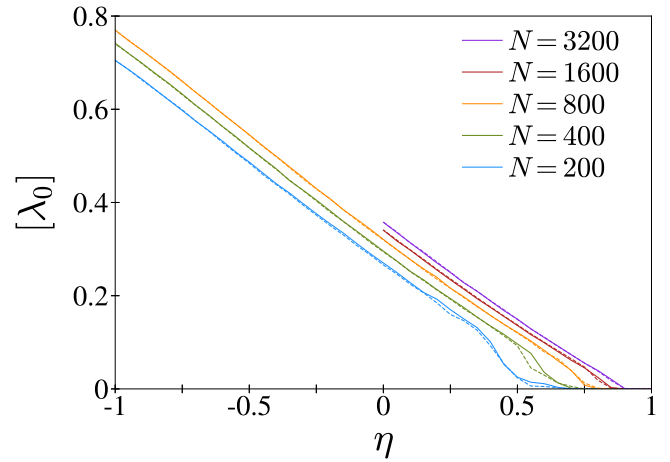


FIG. 3. Largest Lyapunov exponent in the homogeneous limit ($\sigma = 0$), λ_0 versus η for $N = 200, 400, 800, 1600$, and 3200 oscillators. The Lyapunov exponent has been averaged over 20 independent realizations, save for $N = 3200$ with only 10 realizations. Solid (dashed) lines correspond to increasing (decreasing) η .

Lyapunov exponent in the original setup with fixed $\sigma = 1$:

$$\lambda(J \gg 1) \simeq \lambda_0(\eta)J. \quad (14)$$

VI. MODERATE AND STRONG COUPLING

We devote the remainder of this paper to explore the moderate and strong coupling regimes of the DSR model. We first focus on reciprocal coupling, and afterwards the picture is completed studying the general non-reciprocal case.

A. Reciprocal coupling

1. Frequency entrainment and the volcano phase

In the original work by Daido⁵ it is claimed that in the volcano phase, a portion of the oscillators became “quasi-entrained”. By this term, it is meant frequency-entrained, with the phase differences displaying a diffusive drift (i.e. no phase locking). This behavior is quite exotic for a deterministic system, and deserves a deeper scrutiny. The perturbative result in Eq. (9) does not apply, and we resort to direct numerical simulations.

In Fig. 4 (a), we depict the averaged frequencies for $N = 10^4$ oscillators (a fairly large value) and $J = 10$, a coupling strength well above the volcano transition. In the figure we observe oscillators with central natural frequencies settle into averaged frequencies close to zero, but a plateau cannot be distinguished. This would suggest that, in the thermodynamic limit, oscillators with different natural frequencies display different averaged frequencies. The diffusion of the phase difference observed in Ref. 5 is only tangible for short times. In our simulations, we have observed that, for large enough

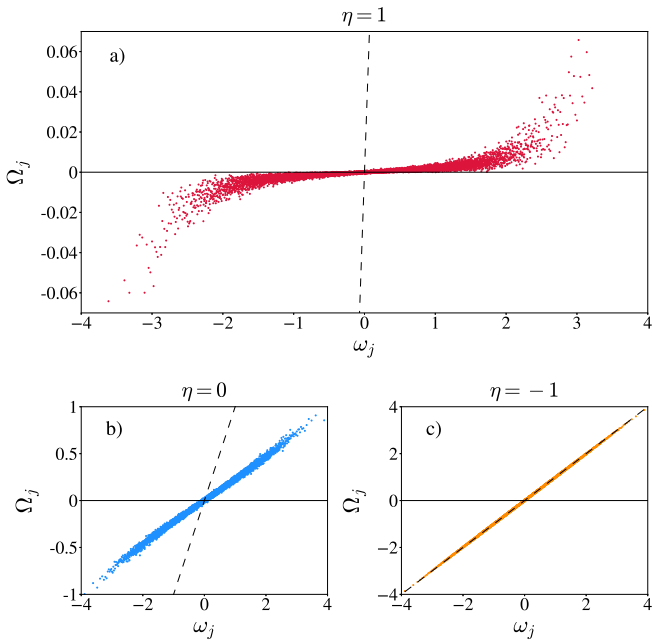


FIG. 4. Long-term average frequencies of a population of 10^4 oscillators with coupling constant $J = 10$, and $\eta = 1, 0$ and -1 in panels (a), (b) and (c), respectively. The time averages were performed over 10^5 t.u. The dashed straight line is $\Omega_j = \omega_j$.

integration times, a ballistic evolution of the phase differences eventually prevails. In other words, frequency entrainment does not emerge with the volcano phase. True phase diffusion would be only possible between oscillators with identical natural frequencies. Because nonreciprocal coupling is less favourable to synchronization, frequency entrainment is not achieved neither for $\eta < 1$, see Figs. 4 (b) and (c). In fact, in the antireciprocal case $\eta = -1$, we observe the averaged frequencies coincide with the natural ones.

2. Multistability and freezing

As already discussed in Sec. III, in the infinite coupling or $\sigma = 0$ limit the system displays a conspicuous multistability of fixed points. Furthermore, according to Stiller and Radons⁶, the system also “freezes” for strong enough coupling. Is freezing concomitant with multistability? Are we even sure that freezing survives in the thermodynamic limit? Our next simulations intend to shed some light on these questions.

In Fig. 5(a) we represent the three largest Lyapunov exponents as a function of the coupling strength for $N = 800$ oscillators, and a particular sample of the coupling matrix elements and the natural frequencies. For every J value, the Lyapunov exponents were computed ten times starting with independent random initial conditions (i.e., ten “replicas” in the jargon of spin glasses). For the largest values of J , we mostly obtain negative Lyapunov exponents, save the first one, which is locked to 0 due to the global rotational symmetry

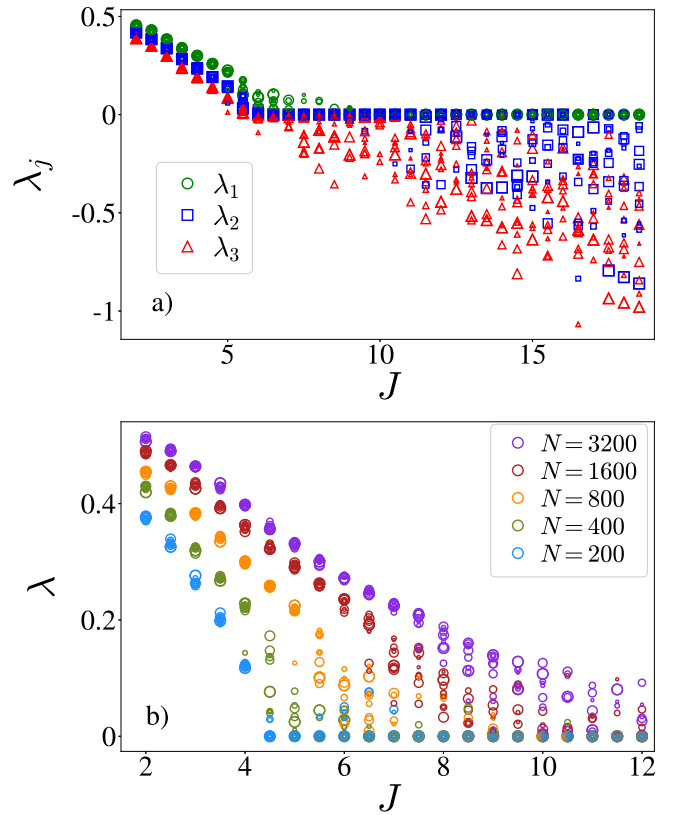


FIG. 5. Lyapunov exponents for one instance of a symmetric coupling matrix K . (a) Three largest Lyapunov exponents $\lambda_1 \geq \lambda_2 \geq \lambda_3$ in green circles, blue squares and red triangles, respectively. The system size is $N = 800$. Ten different initial oscillator phases were implemented for every value of J , and each symbol size corresponds to one of these runs. (b) Largest Lyapunov exponent $\lambda = \lambda_1$ for ten initial conditions, and five system sizes.

$\theta_j \rightarrow \theta_j + \alpha$. The dependence of the negative Lyapunov exponents on the initial condition indicates a multiplicity of resting states (nothing surprising in this context). We also observe values of J where two (or more) exponents are zero. This correspond to states in which most oscillators are entrained to a single frequency, while a few of them are entrained to another frequency, implying quasiperiodicity.

In Fig. 5(a) we may also observe that chaotic and non-chaotic attractors coexist when J is decreased below $J \approx 8$. Eventually, below $J \approx 5$, we infer that only one chaotic attractor survives, as the same Lyapunov exponents are obtained irrespective of the initial condition.

The attentive reader may have noticed that the unentrained state for $J = 10$ in Fig. 4(a) is inconsistent with the resting states found in Fig. 5(a). This apparent discrepancy is due to the disparate population sizes in both figures, $N = 10^4$ vs. $N = 800$. To clarify this issue, we depict the largest Lyapunov exponent for different system sizes in Fig. 5(b). Again, ten random initial conditions are set for every J value. The scenario of panel (a) applies to the other considered population sizes; however, the disappearance of chaos is deferred as N is increased. From our simulations we cannot

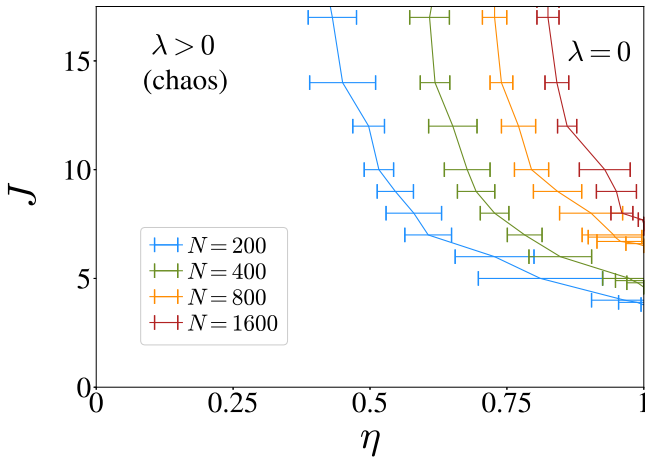


FIG. 6. Partial phase diagram of Eq. (1) for $N = 200, 400, 800$ and 1600 , the solid lines indicate the mean critical value η_c in which the Lyapunov exponent becomes smaller than 10^{-3} . The error bar represent the dispersion among ten realizations of the coupling matrix.

conclude if there is a finite critical $J_c < \infty$ value where chaos ceases in the thermodynamic limit. The freezing transition described in Ref. 6 was claimed to occurs at $J_f \approx 24$ (the value of σ was not specified, but we can presume $\sigma = 1$ as in our case). Our simulations were not able to confirm $J_c \approx J_f$, nor the mere existence of finite J_c and J_f values. At this point, we can only assert that the domain of chaos progressively grows as the system size is increased. Similarly, in Ref. 12 the authors note that, in order to observe the algebraic decay of the order parameter $|Z|$, coupling needed to be progressively increased as $J \sim \sqrt{N}$.

B. Non-reciprocal coupling

Finally, we explore the general non-reciprocal case with non-small coupling. The lack of frequency entrainment was already discussed above. Thus, we focus on the chaotic dynamics.

1. Pervasiveness of Chaos

We now investigate the extension of chaos in the thermodynamic limit. Specifically, we progressively increase the number of oscillators, and determine the region where chaos exists.

In Fig. 6 we show a partial phase diagram for several population sizes. It is obtained computing the largest Lyapunov exponent λ for fixed values of J and N , while, for each realization of the coupling matrix, we vary η . We iteratively detect the value of η at which λ becomes smaller than a threshold value 10^{-3} . This critical $\eta_c(J)$ is averaged over 10 realizations of the coupling matrix. As can be observed, the region with vanishing Lyapunov exponent

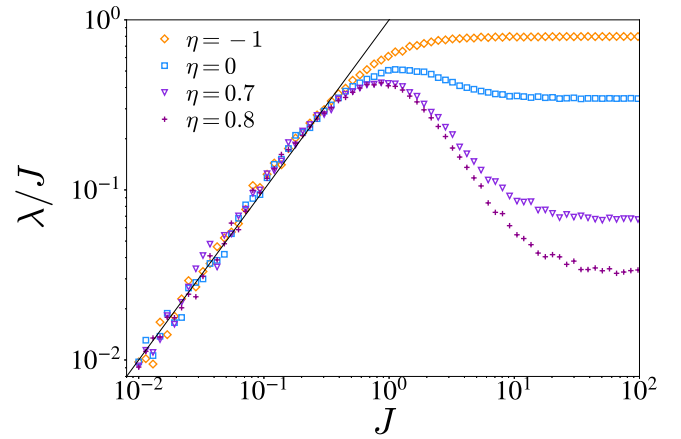


FIG. 7. Largest Lyapunov exponent rescaled by J , λ/J versus J for $N = 2000$ oscillators and different values of η . The black solid line is linear function, showing that the scaling of the exponents for small J values is $\lambda \sim J^2$.

shrinks as N increases. We interpret this result, combined with Fig. 3, as an indication that, in the thermodynamic limit, the system displays non-chaotic behavior only for reciprocal coupling ($\eta = 1$).

The pervasiveness of chaotic attractors when the system size grows is not new in systems with random interactions. In the Kuramoto-Sakaguchi model with random distributed phase lags, recently studied in Ref. 17, increasing the number of oscillators translates into larger basin of attractions of chaotic attractors.

2. Crossover between quadratic to linear growth of $\lambda(J)$

Finally, we study the behavior of the largest Lyapunov exponent with J . In Fig. 7, we depict it rescaled by J for several values of the asymmetry parameter η ($N = 2000$). For small J we observe the quadratic scaling discussed in Sec. IV, while for large values of J , the exponent grows linearly as expected from the simulation in Sec. V. The Lyapunov exponent exhibits an intricate crossover between a quadratic law ($\lambda \sim J^2$) and a linear one ($\lambda \sim J$) as η approaches one. Somehow, the system “feels” the lack of chaos for $\eta = 1$ at $J \rightarrow \infty$. The monotonicity of $\lambda(J)$ is lost at some point in the range $0.7 < \eta < 0.8$.

VII. CONCLUSIONS

In this paper we have studied the dynamics of the fully disordered Kuramoto model (or Daido-Stiller-Radons model^{5,6}) of phase oscillators, Eq. (1). Our work—via numerical simulations and theoretical analysis—sheds light on the dynamics and chaotic properties of the system.

In the weak coupling limit we obtained some analytical results by means of the cavity method. Specifically closed expressions for the long-term average frequencies and the

dissipation were derived using the dynamical cavity method. Both quantities display a strong dependence on the reciprocity parameter η . In contrast, numerical simulations suggest that the first Lyapunov exponent is asymptotically identical for all η values. Elucidating the underlying mechanism for this is an interesting question left for future work.

In the infinite coupling limit, or the identical oscillators case, the DSR model exhibits a glassy phase if the interactions are reciprocal. Incorporating non-reciprocity causes the system to become chaotic. Our simulations, see Fig. 3, suggest that the threshold η value for chaos approaches 1 in the thermodynamic limit.

In the moderate coupling regime, we showed quasientrainment does not occur if large enough integration times and population sizes are considered. We also observed the importance of finite-size effects, since the critical coupling where the system displays freezing strongly depends on N . The exploration of the general non-reciprocal case evidences the pervasiveness of chaos. A peculiar crossover between the quadratic and the linear scalings of the Lyapunov exponent $\lambda(J)$ is uncovered. The value of the asymmetry parameter η determines the shape of the mentioned crossover.

In sum, understanding the significance and the implications of glassy (or quasi-glassy) phases in nonequilibrium systems, from neuroscience to optics, constitutes a fascinating research enterprise³⁸. In this context, the DSR model emerges as a basic prototypical model, since self-sustained oscillators are pervasive in nature and technology. The results presented in this paper may be deemed as limited, but we believe they will pave the way for future progress. As usual in science, our findings also give rise to interesting open problems.

ACKNOWLEDGEMENTS

We acknowledge support by Grant No. PID2021-125543NB-I00, funded by MICIU/AEI/10.13039/501100011033 and by ERDF/EU.

DATA AVAILABILITY

The data that support the findings of this study are available from the corresponding author upon reasonable request.

Appendix A: Dynamical-cavity calculation of the long-term average frequencies and the dissipation

We sketch the dynamical-cavity calculation used to obtain the long-term average frequency and the dissipation in Eqs. (9) and (12), respectively. The derivation is based on the results of Refs. 9 and 10, so we encourage the interested reader to check those references.

As a first step, it is useful to notice that both quantities, the shift of the averaged frequencies and dissipation, can be written in terms of a local quantity M_j related to the local

field (3b):

$$M_j = r_j e^{i(\psi_j - \theta_j)} \quad (\text{A1})$$

The real and imaginary parts, after appropriate averaging, yield:

$$\Omega_j - \omega_j = J \langle \text{Im}(M_j) \rangle_t, \quad (\text{A2})$$

$$\mathcal{S} = -\frac{J}{N} \sum_{j=1}^N \langle \text{Re}(M_j) \rangle_t. \quad (\text{A3})$$

Here $\langle f(t) \rangle_t = \lim_{T \rightarrow \infty} \frac{1}{T} \int_0^T f(t) dt$ is the time average.

The cavity method considers an ensemble of N oscillators and adds another oscillator θ_0 (and its corresponding matrix elements K_{0k} and K_{k0}). Because the new elements are uncorrelated with the evolution of the N previous oscillators, the order parameter $r_0 e^{i\psi_0}$ can be computed by means of the central limit theorem. The evolution of the new oscillators is described (in the thermodynamic limit) by a stochastic equation subject to self-consistent noise^{9,10}:

$$\begin{aligned} \partial_t \theta_0 = \omega_0 + \frac{J}{2i} & \left(e^{-i\theta_0(t)} \xi(t) - e^{i\theta_0(t)} \xi^*(t) \right) \\ & - J^2 \eta \int_0^t dt' R(t, t') \sin(\theta_0(t) - \theta_0(t')) \end{aligned} \quad (\text{A4})$$

In this expression ξ is a complex Gaussian noise, which accounts for the thermodynamic limit of the local field $r_0 e^{i\psi_0}$ in the absence of feedback ($\eta = 0$). The noise ξ has zero mean and the autocorrelations of real and imaginary parts are encoded by these two averages:

$$\langle \xi(t) \xi^*(t') \rangle_\xi = 2C(t, t'), \quad (\text{A5a})$$

$$\langle \xi(t) \xi(t') \rangle_\xi = 0. \quad (\text{A5b})$$

It is simple to calculate C at the lowest order in J ^{9,10} for a Gaussian distribution of frequencies:

$$C(t, t') = \frac{1}{2} e^{-\frac{(t-t')^2}{2}} + O(J^2) \quad (\text{A6})$$

The last term in Eq. (A4) accounts for the feedback effect of the original ensemble (the cavity) on the new oscillator after being perturbed by it. At the lowest order^{9,10}:

$$R(t, t') = H(t - t') \frac{1}{2} e^{-\frac{(t-t')^2}{2}} + O(J^2) \quad (\text{A7})$$

where $H(x)$ is the Heaviside step function.

Hence the local order parameter for oscillator θ_0 at time t (Eq. (35) and (36) in Ref. 10) is:

$$r_0 e^{i\psi_0} = \xi(t) + \eta J \int_0^t e^{i\theta_0(t')} R(t, t') dt' \quad (\text{A8})$$

The dynamics of θ_0 in Eq. (A4) can be perturbatively described by expanding the solution in powers of J : $\theta_0(t) = \theta_0^0 + J\theta_0^1 + \dots$. This yields $\theta_0^0 = \omega_0 t$ and

$$\theta_0^1(t) = \frac{1}{2i} \int_0^t e^{-i\omega_0 t'} \xi(t') - e^{i\omega_0 t'} \xi^*(t') dt'. \quad (\text{A9})$$

If this solution is plugged into Eq. (A8) we get:

$$r_0 e^{i\psi_0} = \xi + \eta J e^{i\omega_0 t} I(t) + O(J^2)$$

where we have defined

$$I(t) = e^{-i\omega_0 t} \frac{1}{2} \int_0^t e^{i\omega_0 t'} e^{-\frac{(t-t')^2}{2}} dt' \quad (\text{A10})$$

With the previous results, we can turn our view to the relevant quantity in Eq. (A1). Up to linear order in J we get

$$\langle M_0 \rangle_t \simeq \langle \xi e^{-i\omega_0 t} - iJ\xi e^{-i\omega_0 t} \theta_0^1(t) + \eta J I(t) \rangle_t \quad (\text{A11})$$

As uncertainties vanish in the thermodynamic limit (self-averagingness), time averages are independent of the realization of the coupling matrix or equivalently the realization of the noise, that is $\langle \rangle_t = \langle \rangle_{t,\xi}$. Thus we evaluate the first two terms in the right hand-side of Eq. (A11):

$$\begin{aligned} \langle \xi(t) e^{-i\omega_0 t} \rangle_t &= \langle \langle \xi(t) \rangle_\xi e^{-i\omega_0 t} \rangle_t = 0 \\ -i \langle \xi(t) e^{-i\omega_0 t} \theta_0^1(t) \rangle_t &= -i \langle e^{-i\omega_0 t} \langle \xi(t) \theta_0^1(t) \rangle_\xi \rangle_t \\ &= \left\langle \int_0^t e^{i\omega_0(t-t')} C(t, t') dt' \right\rangle_t \\ &\simeq \langle I(t) \rangle_t \end{aligned}$$

In the last equality we have used Eqs. (A9) and (A5). Then Eq. (A11) simplifies to:

$$\langle M_0 \rangle_t = (1 + \eta) J \langle I(t) \rangle_t + O(J^3) \quad (\text{A12})$$

It can be shown that terms of order J^2 vanish since an odd number of Gaussian noises need to be averaged in its derivation. The time average of $I(t)$ can be computed

$$\langle I(t) \rangle_t \simeq \sqrt{\frac{\pi}{8}} e^{-\omega_0^2/2} - \frac{i}{\sqrt{2}} D_w(\omega_0/\sqrt{2}) \quad (\text{A13})$$

Inserting this expression into Eq. (A12), and using Eq. (A2) it is straightforward to obtain Eq. (9) in the main text.

To compute \mathcal{S} from Eq. (A3) we need to average over all oscillators. In the thermodynamic limit this is equivalent to average over frequencies, obtaining:

$$\mathcal{S} \simeq -(1 + \eta) J^2 \sqrt{\frac{\pi}{8}} \int_{-\infty}^{\infty} g(\omega) e^{-\omega^2/2} d\omega, \quad (\text{A14})$$

The evaluation of the integral immediately yields Eq. (12) in the main text.

Appendix B: Generation of the coupling matrix

In this appendix we describe how we generate a coupling matrix with cross correlation between symmetric elements given by $\langle K_{jk} K_{kj} \rangle = \eta$. We first build a symmetric matrix S and an antisymmetric matrix A whose elements are drawn from a zero-mean unit-variance normal distribution. The coupling matrix K is computed as:

$$K = \sqrt{\frac{1+\eta}{2}} S + \sqrt{\frac{1-\eta}{2}} A. \quad (\text{B1})$$

By changing η we go continuously from an antisymmetric to a symmetric coupling matrix, as done for Fig. 3 and Fig. 6.

REFERENCES

- ¹A. S. Pikovsky, M. G. Rosenblum, and J. Kurths, *Synchronization, a Universal Concept in Nonlinear Sciences* (Cambridge University Press, Cambridge, 2001).
- ²Y. Kuramoto, *Chemical Oscillations, Waves, and Turbulence* (Springer-Verlag, Berlin, 1984).
- ³Y. Kuramoto, "Self-entrainment of a population of coupled non-linear oscillators," in *International Symposium on Mathematical Problems in Theoretical Physics*, Lecture Notes in Physics, Vol. 39, edited by H. Araki (Springer, Berlin, 1975) pp. 420–422.
- ⁴D. Sherrington and S. Kirkpatrick, "Solvable model of a spin-glass," *Phys. Rev. Lett.* **35**, 1792–1796 (1975).
- ⁵H. Daido, "Quasientrainment and slow relaxation in a population of oscillators with random and frustrated interactions," *Phys. Rev. Lett.* **68**, 1073–1076 (1992).
- ⁶J. C. Stiller and G. Radons, "Dynamics of nonlinear oscillators with random interactions," *Phys. Rev. E* **58**, 1789–1799 (1998).
- ⁷J. P. L. Hatchett and T. Uezu, "Mean field and cavity analysis for coupled oscillator networks," *Phys. Rev. E* **78**, 036106 (2008).
- ⁸T. Kimoto and T. Uezu, "Correspondence between phase oscillator network and classical XY model with the same random and frustrated interactions," *Phys. Rev. E* **100**, 022213 (2019).
- ⁹A. Prüser, S. Rosmej, and A. Engel, "Nature of the volcano transition in the fully disordered Kuramoto model," *Phys. Rev. Lett.* **132**, 187201 (2024).
- ¹⁰A. Prüser and A. Engel, "Role of coupling asymmetry in the fully disordered Kuramoto model," *Phys. Rev. E* **110**, 064214 (2024).
- ¹¹D. Pazó and R. Gallego, "Volcano transition in populations of phase oscillators with random nonreciprocal interactions," *Phys. Rev. E* **108**, 014202 (2023).
- ¹²Z. G. Nicolaou, H. Cho, Y. Zhang, J. N. Kutz, and S. L. Brunton, "Signature of glassy dynamics in dynamic modes decompositions," (2025), arXiv:2502.10918 [cond-mat.dis-nn].
- ¹³E. Montbrió and D. Pazó, "Shear diversity prevents collective synchronization," *Phys. Rev. Lett.* **106**, 254101 (2011).
- ¹⁴D. Pazó and E. Montbrió, "The Kuramoto model with distributed shear," *EPL (Europhys. Lett.)* **95**, 60007 (2011).
- ¹⁵E. Montbrió and D. Pazó, "Collective synchronization in the presence of reactive coupling and shear diversity," *Phys. Rev. E* **84**, 046206 (2011).
- ¹⁶D. Iatsenko, P. V. E. McClintock, and A. Stefanovska, "Oscillator glass in the generalized Kuramoto model: synchronous disorder and two-step relaxation," *Nat. Commun.* **5**, 4188 (2014).
- ¹⁷A. Pikovsky and F. Bagnoli, "Dynamics of oscillator populations with disorder in the coupling phase shifts," *New J. Phys.* **26**, 025054 (2024).
- ¹⁸L. A. Smirnov and A. Pikovsky, "Dynamics of oscillator populations globally coupled with distributed phase shifts," *Phys. Rev. Lett.* **132**, 107401 (2024).
- ¹⁹F. A. Rodrigues, T. K. D. Peron, P. Ji, and J. Kurths, "The Kuramoto model in complex networks," *Physics Reports* **610**, 1–98 (2016).
- ²⁰H. Chiba and G. S. Medvedev, "The mean field analysis of the Kuramoto model on graphs I. the mean field equation and transition point formulas," *Discrete Contin. Dyn. Syst. Ser. A* **39**, 131–155 (2019).
- ²¹P. Villegas, P. Moretti, and M. A. Munoz, "Frustrated hierarchical synchronization and emergent complexity in the human connectome network," *Sci. Rep.* **4**, 5990 (2014).
- ²²H. Daido, "Algebraic relaxation of an order parameter in randomly coupled limit-cycle oscillators," *Phys. Rev. E* **61**, 2145–2147 (2000).
- ²³J. C. Stiller and G. Radons, "Self-averaging of an order parameter in randomly coupled limit-cycle oscillators," *Phys. Rev. E* **61**, 2148–2149 (2000).
- ²⁴B. Ottino-Löffler and S. H. Strogatz, "Volcano transition in a solvable model of frustrated oscillators," *Phys. Rev. Lett.* **120**, 264102 (2018).
- ²⁵P. Spitzner and W. Kinzel, "Freezing transition in asymmetric random neural networks with deterministic dynamics," *Zeitschrift für Physik B Condensed Matter* **77**, 511–517 (1989).
- ²⁶H. Eissfeller and M. Opper, "Mean-field Monte Carlo approach to the Sherrington-Kirkpatrick model with asymmetric couplings," *Phys. Rev. E* **50**, 709–720 (1994).

- ²⁷A. Crisanti and H. Sompolinsky, “Dynamics of spin systems with randomly asymmetric bonds: Langevin dynamics and a spherical model,” *Phys. Rev. A* **36**, 4922–4939 (1987).
- ²⁸M. Mézard, G. Parisi, and M. A. Virasoro, *Spin glass theory and beyond: An Introduction to the Replica Method and Its Applications*, World Scientific Lecture Notes in Physics, Vol. 9 (World Scientific Publishing Company, Singapore, 1987).
- ²⁹H. Daido, “Superslow relaxation in identical phase oscillators with random and frustrated interactions,” *Chaos* **28**, 045102 (2018).
- ³⁰O. V. Popovych, Y. L. Maistrenko, and P. A. Tass, “Phase chaos in coupled oscillators,” *Phys. Rev. E* **71**, 065201(R) (2005).
- ³¹Y. Kati, J. Ranft, and B. Lindner, “Self-consistent autocorrelation of a disordered kuramoto model in the asynchronous state,” *Phys. Rev. E* **110**, 054301 (2024).
- ³²L. Bonilla, C. Pérez Vicente, and J. Rubí, “Glassy synchronization in a population of coupled oscillators,” *J. Stat. Phys.* **70**, 921–937 (1993).
- ³³A. Pikovsky and A. Politi, *Lyapunov Exponents: A Tool to Explore Complex Dynamics* (Cambridge University Press, 2016).
- ³⁴M. Carlu, F. Ginelli, and A. Politi, “Origin and scaling of chaos in weakly coupled phase oscillators,” *Phys. Rev. E* **97**, 012203 (2018).
- ³⁵M. Carlu, *Instability in high-dimensional chaotic systems* (Thesis (Ph.D.)–Aberdeen University, 2019, 2019).
- ³⁶R. Hanai, “Nonreciprocal frustration: Time crystalline order-by-disorder phenomenon and a spin-glass-like state,” *Phys. Rev. X* **14**, 011029 (2024).
- ³⁷Z. Liu, Y.-C. Lai, and M. A. Matías, “Universal scaling of lyapunov exponents in coupled chaotic oscillators,” *Phys. Rev. E* **67**, 045203 (2003).
- ³⁸P. Charbonneau, E. Marinari, M. Mézard, G. Parisi, F. Ricci-Tersenghi, G. Sicuro, and F. Zamponi, *Spin glass theory and far beyond: replica symmetry breaking after 40 years* (World Scientific, Singapore, 2023).